The Model Calculation of Angular Dependence of CESR Linewidth in Aluminium

Andrei B. Bondarenko, Yurii N. Proshin
Kazan State University, Kremlevskaya, 18, Kazan 420008, Russia
E-mail: Yurii.Proshin@ksu.ru

Received June 30, 1997
Revised July 15, 1997
Accepted July 25, 1997

Volume **1**
No. **1, 1997**

Abstract

A simple model of the Fermi surface for the interpretation of the conduction electron spin resonance (CESR) results in aluminium is developed. According to the real aluminium Fermi surface 48 small circles with the large amount of the g-factor shift are arranged in five layers on the Fermi sphere, as distinct from the random distribution of them in the previous model proposed by Silsbee and Beuneu (SB). The present model reproduces the known experimental CESR linewidth dependencies versus the frequency at different temperature region as well as the SB model. Additionally to the SB results the CESR linewidth is found to be independent from the magnetic field direction in the high temperature approximation. In both other cases (intermediate and low temperatures) the g-value anisotropy over Fermi surface is predicted to lead to the essential angular CESR linewidth dependence with five peaks. Some applications of the model to various systems with conduction electrons are discussed.

PACS : 76.30.Pk; 71.18.+y

Keywords : conduction electrons, Fermi surface, spin resonance, aluminium

1 Introduction.

The angular dependence of the conduction electron spin resonance (CESR) can be caused by the influence of sample boundaries. It is often considered as the sole cause in the treatment of experimental data, especially for thin metallic films [1, 2]. The appearance of the CESR angular dependence may be also connected with the Fermi surface anisotropy and (or) conduction electrons g-factor spread over the Fermi surface [3]. Together with magnetic breakdown [4, 5, 6] this must be taken into account for the metallic specimens with monocrystal or oriented polycrystal structure.

In this paper we advance a simple model of such anisotropy and we believe that the model can work not only for usual polyvalent metals with complicated Fermi surface (Al, Be, Mg, Zn, *etc.*), but it also may be useful for the interpretation of the CESR data for modern materials (organic conductors [7], for example). The model is appreciable founded on the one proposed by Silsbee and Beuneu (SB) [8] to explain the CESR linewidth linear dependence on frequency in terms of the motional narrowing within the intermediate temperature range.

It is known [6, 9, 10] that the conduction electrons with different quasimomenta $\mathbf{p}$ have different g-factor: $g(\mathbf{p})$. The difference between the conduction electron g-factor and the free electron value g_0 arises due to the spin-orbit coupling. Beuneu [12] calculated explicitly the conduction electron g-factor for aluminium in more than 8000 points on the Fermi surface, thus he determined the $\mathbf{p}$-dependence of the g-shift

$$\delta g(\mathbf{p}) = g(\mathbf{p}) - \langle g(\mathbf{p}) \rangle \equiv g(\mathbf{p}) - g. \tag{1}$$

Here $\langle ... \rangle$ means standard average on the Fermi surface.

A remarkable feature of this calculation is the existence of very long tails in the spread of g-shift, which extend to values of δg as large as plus and minus several hundreds.

The appearance of these very large g-shifts is a natural consequence of the existence of 24 degeneracy points on the free electron approximation Fermi surface where the second and third zones contact [11]. Al is a metal with a face-centered cubic lattice and a cubical octahedron Brillouin zone. These points (W-points) are localised on the intersections of quadrangular and hexangular faces (see Fig.1). Here the g-factor can achieve the value of several hundreds. This circumstance was taken into account in the following way [8]. Spin-orbit interaction lifts the degeneracy and small spin-orbit gap gives rise to locally very small effective masses and hence to exceedingly large orbital moments which, in turn, are strongly coupled to the spin [9]. There are 48 small spots with large g-shifts on the Fermi surface of aluminium in the vicinity of the W-points, 24 ones on each of the second- and third-zone surfaces, after lifting of the degeneracy by the spin-orbit splitting. The role of g anisotropy in clarifying experimental CESR linewidth dependencies versus the frequency at different temperatures for Al has been explored theoretically by Beuneu [12], SB [8]. Freedman and

Fredkin [13], Silsbee and Long [14] have investigated combined effects of an exchange and the g anisotropy.

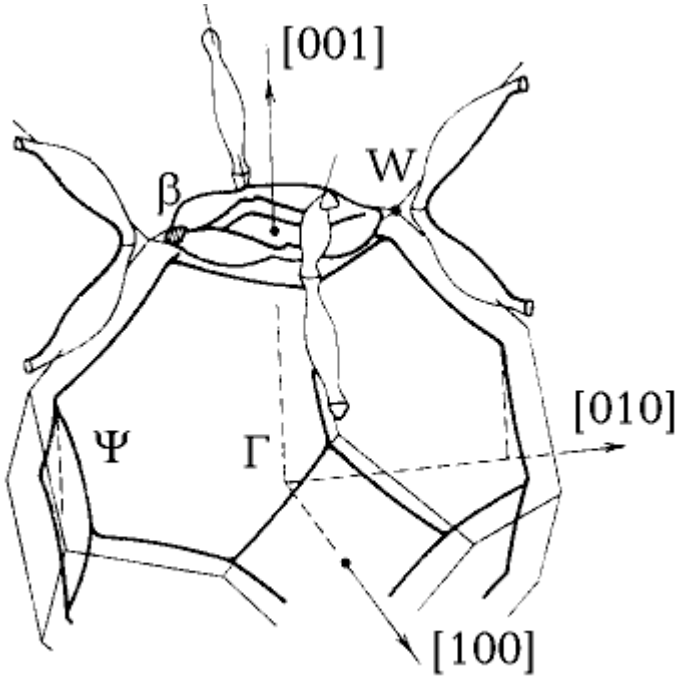

Figure 1: The real Fermi surface and the Brillouin zone for aluminium.

As regard to the magnetic breakdown, it provides a contribution to the full CESR linewidth with the g-anisotropy existence only [4], [5]. The calculations [5, 6] have showed that this contribution is directly proportional to the magnetic breakdown probabilities. In turn, these probabilities are known to depend on the magnetic field inclination angle. Hence this dependence is extended to the CESR linewidth.

To conclude this section let us mention that the number of references incorporating the real Fermi surface structure of metals for the CESR research may be found in the recent review [6].

2 Model discussion.

Assuming that all mechanisms of a broadening and a shift of the CESR line give additive contributions, we will consider in more detail the contribution of indicated anisotropy $g(\mathbf{p})$ distribution over the Fermi surface to the angular dependence of the CESR linewidth. We will neglect all other causes of spin lifetime

shortening due to the scattering on other electrons, phonons, boundaries, impurities, dislocations and inhomogeneities of other kinds leading to homogeneous linewidth of CESR.

The simplest interpretation of the observed line width is as follows. The conduction electrons with different quasi-momenta (and different g-factors) should be in resonance with different fields. Hence, if it were possible to observe, the experiment would exhibit an inhomogeneous CESR line profile corresponding to the real spread of the electron g-factor over the Fermi surface

$$\Delta\omega_g \simeq \frac{1}{\hbar}\sigma_g \mu_{\rm B} H. \tag{2}$$

Here $\sigma_g = \left\langle (\delta g)^2 \right\rangle^{1/2}$ is the mean square deviation of the g-factor over the Fermi surface, $\mu_{\rm B}$ is the Bohr magneton. In this case $\Delta\omega_g$ is the CESR linewidth due to the g anisotropy.

In reality, such an inhomogeneously broadened line is not observable. The reason is that the conduction electrons do not "stand still" at different places on the Fermi surface. In a magnetic field the conduction electrons move over the Fermi surface either along cyclotron orbits (high fields, low temperatures, pure metals), or in a diffusive mode because of all kinds of scattering mechanisms (by convention we will call this case a "high temperature" one). In the second case the magnetic field influence on the electrons motion over the Fermi surface is negligible.

In the high temperature case the conduction electron is able to "visit" many points over the Fermi surface during spin lifetime τ_s because of $\tau_s \gg \tau$ where τ is scattering momentum time, characterising the transition from one $\mathbf{p}$ state on Fermi surface to another one. These various points are characterised by different g-factors $g(\mathbf{p})$ and different local resonance fields H, correspondingly (as a rule the CESR spectrometers operate at a fixed frequency ω_s). As a result the conduction electrons experience the action of a somewhat averaged field, and the CESR line becomes narrower. The corresponding contribution of the g-factor anisotropy to the linewidth is given by the known formula of "motional narrowing"

$$\Delta\omega \sim \frac{\sigma_g^2}{g^2}\omega_s^2 \tau. \tag{3}$$

Here ω_s is the resonance frequency.

In rather pure metals the temperature decreasing causes an increase in the conduction electron momentum relaxation time τ. The contribution to the linewidth (3) also rises. This rise can go on until τ^{-1} becomes of the order of $\Delta\omega_g$. However before the full breakdown of motional narrowing the conduction electrons start to move along cyclotron orbits. In this situation an electron can manage to accomplish several revolutions around the Fermi surface between two scattering events because the cyclotron frequency ω_c becomes larger than τ^{-1}.

Under this condition the g-factor must be averaged over the cyclotron orbits at first.

For each orbit characterised by p_z there is its g-factor shift [12, 13] (magnetic field $\mathbf{H}$ is directed parallel to z axis)

$$\Delta g(p_z) = \langle g(\mathbf{p}) \rangle_{p_z = \text{const}} - \langle g(\mathbf{p}) \rangle \ .$$

This shift significantly reduces the g-factor mean square spread σ_g which is equal to $\left\langle (\Delta g(p_z))^2 \right\rangle^{1/2}$ for the considered case. For instance, in Al the g-factor averaging over all the Fermi surface due to the conduction electron diffusive motion yields $\sigma_g = 0.469$, while the initial averaging over cyclotron orbits can reduce this spread down to $\sigma_g = 0.067$ [12]. In the most interesting intermediate case ($\omega_c \tau \sim 1$) the averaging procedure should be very sophisticated due to the mixed nature of conduction electron motion in magnetic field (see below) and the real Fermi surface computations have not been carried out [12].

The present research is devoted to the development of a model proposed by SB [8] for the CESR linewidth behaviour interpretation in aluminium. Briefly we will point out the main features of the SB model. The conduction electrons were taken as a free electron gas. Instead of the real complicated Fermi surface with actual g-spread they suggested to consider the Fermi sphere lying in several Brillouin zones. The radius of Fermi sphere is p_{F}. This procedure may be named inverse reconstruction of Harrison. Almost anywhere on the Fermi sphere the g-factor was taken to be equal to g (see Eq.(1)), that was calculated by Beuneu [12]. The 48 small circular areas (named as R-disks) with the large g-shift were corresponded to the nearest neighbourhoods of W-points

$$|\delta g_0| = 1.1 \cdot 10^3.$$

This shift was taken positive on one-half of the R-disks, negative on the rest, to leave a mean g-shift of zero. The radius of the R-disks was appropriately taken to give a disk area πp^2 equal to the area, near the W-points of the real Fermi surface in aluminium over which the energy gap is dominantly determined by the spin-orbit interaction

$$p = 0.7 \cdot 10^{-3} p_{\mathrm{F}}.$$

Thus, σ_q calculated on the sphere was equal to 2.7. To simplify the calculations SB supposed that the 48 R-disks were RANDOMLY distributed over the sphere. Naturally, owing to this assumption the possible linewidth anisotropy was omitted from the model.

Our model differs from the above mentioned one by a REGULAR ARRANGEMENT of the R-disks on the Fermi sphere. This disposition of the R-disks corresponds most closely to the arrangement of the W-points neighbourhoods on the real Fermi surface.

Using the reverse reconstruction of Harrison we obtain that 48 R-disks are arranged in 5 layers (see Fig.2): 16 disks are in equatorial one and 8 disks are

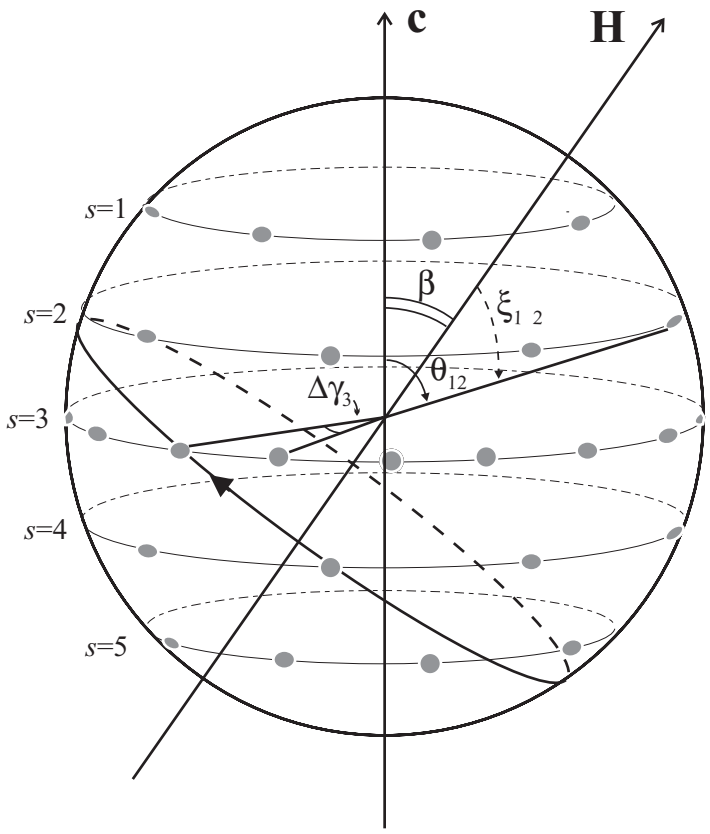

Figure 2: The schematic view of the free-electron Fermi surface in aluminium with R-disks (the shaded areas). The direction of conduction electron movement is shown by arrow. The characteristic angles used in our calculations are indicated.

in each of the remaining ones. The appropriate angles on the R-disks levels are equal to θ_i

$$\begin{array}{c} \theta_{1,\ldots,8} = \arctan(1/2) \\ \theta_{9,\ldots,16} = \pi/2 - \arctan(1/2) \\ \theta_{17,\ldots,32} = \pi/2 \\ \theta_{33,\ldots,40} = \pi/2 + \arctan(1/2) \\ \theta_{41,\ldots,48} = \pi - \arctan(1/2). \end{array} \tag{4}$$

Individual electrons are assumed to be scattered randomly from point to point on the Fermi sphere at rate $1/\tau$. Between scattering events they move along cyclotron orbits on the Fermi sphere with a linear velocity in quasimomentum space,

$$|\dot{\mathbf{p}}| = \omega_c p_{\mathrm{F}} \sin\theta,$$

where θ is the angle between the electron quasimomentum $\mathbf{p}$ and the applied field $\mathbf{H}(0,0,H)$.

Now we can use the analytical "motional narrowing" procedure of the initial g-factor distribution with reasonable facility.

3 The CESR linewidth calculations for model Fermi surface.

The main parameter of the proposed theory is the magnitude of the typical orbital segment length in $\mathbf{p}$-space, $\omega_c \tau p_{\mathrm{F}}$, traversed by an electron along cyclotron orbit between scattering events. This parameter determines the manner in which motional narrowed linewidth arises. There are three different temperature regimes defined by $\omega_c \tau p_{\mathrm{F}}$. In the high-temperature region (case A) the conduction electrons are scattered on and off the R-disks more rapidly than they move on and off the disks because of their cyclotron motion, and hence the effects of cyclotron motion are negligible. An electron has no time to cross completely the R-disk along cyclotron orbit before the next scattering event

$$\omega_c \tau p_{\mathrm{F}} \ll p.$$

In the low temperature regime (case C) the conduction electron, on the contrary, can make few revolutions along a single cyclotron orbit before scattering to a new orbit

$$\omega_c \tau \gg 1.$$

The cyclotron motion now gives effective averaging over the full orbit of the g variation associated with all traversed R-disks.

The virtue of the present model is the possibility of averaging in an intermediate temperature regime (case B)

$$p \ll \omega_c \tau p_{\mathrm{F}} \ll p_{\mathrm{F}}.$$

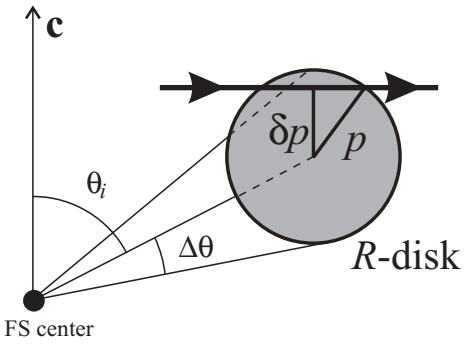

Figure 3: The R-disk (the shade area). θ_i is the angle on the R-disk, δp is the impact parameter, the line with arrows indicates the direction of the conduction electrons movement.

Under these conditions the conduction electron passes along cyclotron orbit a distance larger than a size of the R-disk. It may cross either no or one or several R-disks completely, but it has no time ($\tau < \omega_c$) to make even one revolution along a single cyclotron orbit.

The correlation time for the narrowing is determined not by the time between collisions, but the average time spent on the R-disks, which is now determined only by the speed of the cyclotron orbital motion, not the collision rate. The time τ in Eq.(3) must be replaced by the disk transit time, which is approximately equal to $p/(p_{\rm F}\omega_c)$. As noted by SB, in this regime the linewidth varies as ω_s^2/ω_c and is therefore linearly proportional to the field at which the experiment is performed, and a natural explanation is obtained for the experimentally observed linear dependence of linewidth upon frequency.

Note the conclusions of SB about the frequency and temperature dependence of the CESR linewidth in aluminium are valid for our model. Therefore we focus our attention on those new outcomes, which could not be obtained in indicated work. To clarify this difference we will not change all parameters introduced by SB: $\delta g_0, p, g, p_{\rm F}, \omega_c$, etc.

In the high-temperature regime (case A) the conventional result for motional narrowing is appropriate (3). The linewidth does not depend upon the magnetic field inclination angle β. We have the SB result

$$\left\langle (\delta g)^2 \right\rangle = (\delta g_0)^2 \left(48\pi p^2/4\pi p_{\rm F}^2\right)$$

$$A)\ \Delta\omega^{(\rm A)} = \Delta\omega_{\rm SB}^{(\rm A)} = 12\left(\frac{\delta g_0}{g}\frac{p}{p_{\rm F}}\omega_s\right)^2 \cdot \tau \equiv 12F^2\tau \qquad (5)$$

with parameter $F = (\delta g_0/g)(p/p_{\rm F})\omega_s$. Here and below $\Delta\omega$ denotes the contribution of the motional averaged g anisotropy to the full CESR linewidth $1/T_2$,

assuming a scalar g-shift rather than the tensor. Taking into account g-tensor properties leads to an appearance of a correction factor of 2 [8, 15] in all the linewidth expressions, see Eqs.(5), (10) and (15).

Firstly we examine our system for a case of $\mathbf{H}\|\mathbf{c}$.

In intermediate temperature region (case B) we have to take into account the peculiar character of the conduction electrons movement.

Following SB the spin precession phase of an electron passed through the R-disk relative to the mean phase of all of the spins is written as

$$\phi(\theta, \delta p) = \left[\frac{\delta g_0}{g}\omega_s\right] \frac{2\left(p^2 - \delta p^2\right)^{\frac{1}{2}}}{\omega_c p_{\mathrm{F}} \sin\theta} \tag{6}$$

where θ is angle of orbit, δp is impact parameter (see Fig.3).

Let us determine the rate at which any given electron moving along the orbit with polar angle θ meets R-disk

$$R(\theta) = \begin{cases} \omega_c p_{\mathrm{F}} \sin\theta \times 2p_{\mathrm{F}}/(4\pi p \sin\theta_i^{'}), \text{ if } \theta \in (\theta_{\mathrm{i}} - \Delta\theta, \theta_{\mathrm{i}} + \Delta\theta) \\ 0, \text{ if } \theta \notin (\theta_{\mathrm{i}} - \Delta\theta, \theta_{\mathrm{i}} + \Delta\theta) \end{cases}, \tag{7}$$

where the angle $\theta_i^{'}$ is equal to $\arcsin\left(\left(\sin\left(\theta_i - \Delta\theta\right) + \sin\left(\theta_i + \Delta\theta\right)\right)/2\right)$, θ_i is a mean angle on the $R-$disk level, $\Delta\theta = 2\arcsin\left(p/p_{\mathrm{F}}\right)$, $2p$ is the collision cross section.

Using the fact that the rate at which the electrons gain the mean-square precession phase error is then given by

$$\frac{d}{dt}\left\langle\phi^2(t)\right\rangle = \frac{1}{4\pi}\int_0^{\pi} 2\pi R(\theta)\sin\theta\left\langle\phi^2(\theta, \delta p)\right\rangle_{\delta p} d\theta \tag{8}$$

and with the result of SB

$$\Delta\omega = \frac{1}{2}\frac{d}{dt}\left\langle\phi^2(t)\right\rangle, \tag{9}$$

where $\langle ... \rangle_{\delta p}$ is the average $\phi(\theta, \delta p)$ over impact parameters $(-p \le \delta p \le p)$, we get

$$B)\ \Delta\omega^{(B)} = \frac{F^2\Delta\theta}{24\omega_c}\sum_{i=1}^{48}\frac{1}{\sin\theta_i} \tag{10}$$

with a parameter $\Delta\theta \simeq 2p/p_{\mathrm{F}}$. The SB result differs from expression (10) and may be written as

$$\Delta\omega_{\mathrm{SB}}^{(B)} = \frac{12F^2}{\omega_c}\left(\frac{p}{p_{\mathrm{F}}}\right). \tag{11}$$

As a next step, let us consider the low temperature case. The CESR linewidth is given by Eq.(3) and

$$\delta g(\theta, \delta p) = \delta g_0 \frac{2\left(p^2 - \delta p^2\right)^{\frac{1}{2}}}{2\pi p_{\rm F} \sin\theta}. \tag{12}$$

The probability that the orbit with polar angle θ in this case traverses a R-disk is

$$P(\theta) = \begin{cases} 1, \text{ if } \theta \in (\theta_{\rm i} - \Delta\theta, \theta_{\rm i} + \Delta\theta)\ , \ {\rm i} = 1, 2, ..., 48 \\ 0, \text{ if } \theta \notin (\theta_{\rm i} - \Delta\theta, \theta_{\rm i} + \Delta\theta)\ , \ {\rm i} = 1, 2, ..., 48 \end{cases}. \tag{13}$$

Defining the mean-square deviation of $g(p)$ from its mean value g

$$\left\langle [\delta g(\theta, \delta p)]^2 \right\rangle = \frac{1}{4\pi} \int\limits_0^\pi 2\pi P(\theta) \sin\theta d\theta \left\langle [\delta g(\theta, \delta p)]^2 \right\rangle_{\delta p}\ , \tag{14}$$

we obtain by a straightforward calculation

$$C)\ \Delta\omega^{\rm (C)} = \frac{{\rm F}^2\tau}{6\pi^2} \sum_{\rm i=1}^{48} \ln \frac{\tan\left(\theta_{\rm i}'/2\right)}{\tan\left(\theta_{\rm i}''/2\right)} \simeq \frac{{\rm F}^2\tau\Delta\theta}{3\pi^2} \sum_{\rm i=1}^{48} \frac{1}{\sin\theta_{\rm i}} \tag{15}$$

with $\theta_{i'(i'')} = \theta_i \pm \Delta\theta$. SB have obtained

$$\Delta\omega_{\rm SB}^{(C)} = \frac{12F^2}{\tau} \left(\frac{p}{p_{\rm F}}\right). \tag{16}$$

The expressions (10), (15) are valid for the case of $\mathbf{H} \| \mathbf{c}$ or $\beta = 0$ ($\mathbf{c}$ is the symmetry axis of crystal, see Fig.2). For arbitrary angle of the magnetic field tilt it is necessary to substitute ξ_i instead of θ_i into equations (7)–(15), where ξ_i are found from next relationship

$$\cos\xi_i = \cos\theta_i \cos\beta - \sin\theta_i \sin\beta \cos\gamma_i \tag{17}$$

here $\gamma_i = \gamma^s + m\Delta\gamma_s$ is the angle in the plane of the R-disks layer with number $s = s(i)$ (see Fig.2). γ^s is the polar angle defining the magnetic field direction relative to the R-disk with $m = 0$ ($\gamma^2 = \gamma^4 = \gamma^1 + \pi/8 = \gamma^3 + \pi/8 = \gamma^5 + \pi/8$), $m = m(i) = 0, 1, 2, \ldots$ is the number of R-disk on a given layer, $\Delta\gamma_3 = \pi/8$ for equatorial level and $\Delta\gamma_s = \pi/4$ for remaining ones.

Note, the expressions (10) and (15) in the case $0 \leq \xi_i \leq \Delta\theta$ do not give a good result, because expression (6) cannot be used. In this case we must use the simple expression (3) with $g = \delta g_0$.

The linewidth dependence upon the magnetic field inclination angle β is calculated for typical values of $\omega_c\tau$ and corresponding curves are represented in Fig.4.

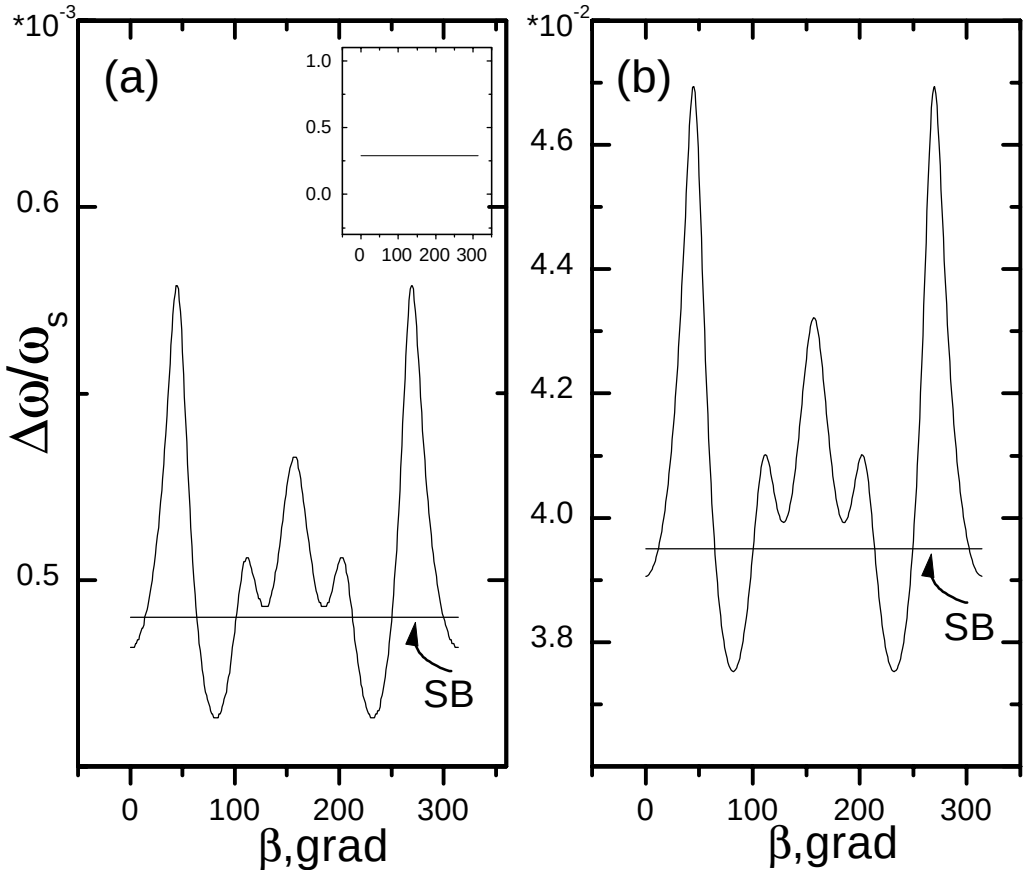

Figure 4: The theoretical CESR linewidth of aluminium versus angle β calculated with Eqs. (5), (10), (15) a) The low temperature regime. On the inset there is the high temperature regime line. b) The intermediate temperature regime.

4 Discussion and conclusions.

Let us summarise.

In the high temperature region the linewidth is independent from the magnetic field direction. The conduction electrons diffusion over Fermi surface is caused by various mechanisms of scattering. It makes insufficient a consideration of comprehensive structure of the Fermi surface and our results coincide completely with the SB ones. Both results are shown in the inset at the right upper corner of the Fig.4).

Two other cases are more interesting.

In the intermediate temperature region there are characteristic peaks at values of β coinciding with appropriate angles determined by Eq. (4), (see Fig.4-b). If we average expression (10) on the angle β, we can obtain approximately the same result that could be directly derived from the SB expression (11)

$$\frac{1}{\pi}\int_0^{\pi}\Delta\omega(\beta)d\beta \approx \Delta\omega_{\rm SB}. \tag{18}$$

In the low temperature region the angle dependence is represented on the Fig.4a). The mean value (18) coincides numerically with corresponding value of the SB.

On the Fig.5 we represent the calculated CESR linewidth of aluminium versus angle β for different values γ_i. Obviously, the linewidth dependence on γ_i is symmetric relatively $\pi/8$ and periodic with the period of $\pi/4$. We also observe a symmetry of the shape of curves relatively the angle $\beta = \pi/2$. There are five peaks within the β range $(0,\ \pi)$ on angles coinciding with ones determined by right sides expression (4). The peaks, which correspond angles $\beta = \pi/2 \pm \arctan(1/2)$, are weakly expressed on angles $\gamma_1 \simeq 0,\ \pi/8$, the ones have a maximum for angle $\gamma_1 = \pi/4$. The intensity of the peaks corresponding angles $\beta = \arctan(1/2)$ and $\beta = \pi - \arctan(1/2)$ have inverse dependence.

To evaluate the temperature dependence of the CESR linewidth at high temperatures we have to take into account the phonon-induced relaxation. Since we have no difference with the model of SB in this regime, we will reproduce their estimation of the phonon-induced contribution to the CESR linewidth, $\Delta\omega_{ph}$ below.

More detail estimation using the real Fermi surface structure near the W-points yields $\Delta\omega_{ph} = 1.5\cdot 10^{-4}/\tau$. The resultant expression for $\Delta\omega_{ph}$ determined from the fit with experimental data [8] is

$$\Delta\omega_{ph} = \frac{1.5\cdot 10^{-4}}{\tau} \tag{19}$$

Thus, at high temperatures we have two contributions to the CESR linewidth caused by g anisotropy (5) and (19)

$$\Delta\omega_g^{(A)} = \Delta\omega^{(A)} + \Delta\omega_{ph}. \tag{20}$$

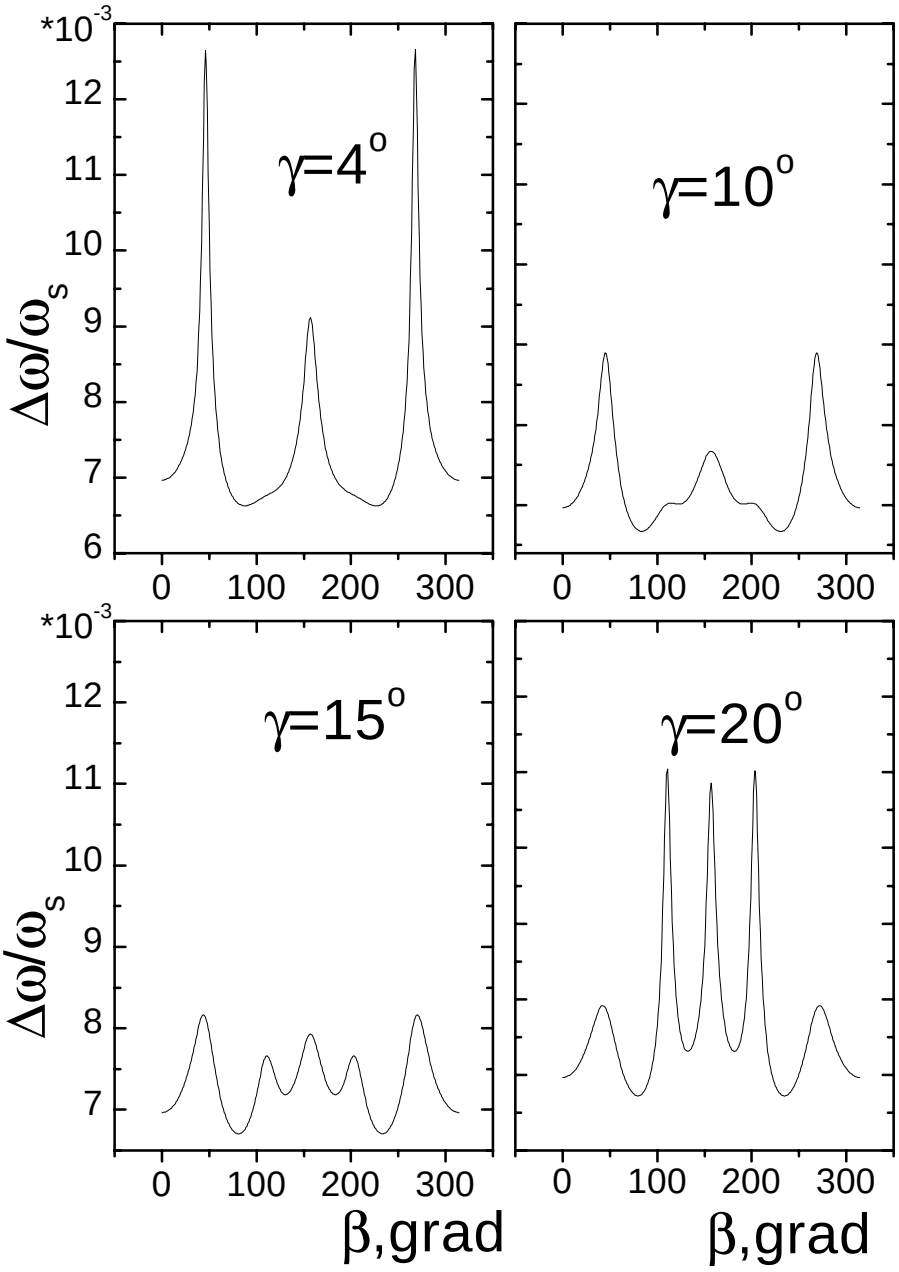

Figure 5: The CESR linewidth as a function of angle β. Our model predicts various behaviours for different values of the angle $\gamma = \gamma_1$.

The scattering rate, τ, is determined by the phonon one. It is well known, that the last value varies as T^3

$$\frac{1}{\tau} = pT^3.$$

The theoretical fit [8] has yielded $p = 2.1 \cdot 10^7 \mathrm{sec}^{-1}\mathrm{K}^{-3}$.

The temperature dependence of the CESR linewidth (or dependence upon $\omega_c\tau$) is calculated using the equations (10), (15), (20) and it has qualitatively the same character as the dependence of SB. Naturally, we have the close agreement for the average values of Eq. (18) and we must use this dependence for polycrystal nonoriented samples.

There are the following main experimental features (see corresponding figure from the SB work).

1) At high temperatures the experimental dependence of linewidth ($\sim T^3$) is reproduced by (20). An apparent frequency dependence of the phonon spin-flip scattering can be understood as a consequence of the motional narrowing model, with the phonon-induced relaxation remaining independent of frequency.

2) There is the linewidth minimum at the intermediate temperatures. And the minimum linewidth depends linearly on frequency, as indicated by (10).

The linewidth behaviour with temperature in our model agrees qualitatively to experimental data too. For an extended discussion see mentioned paper of SB [8].

Note a gap between estimated and observed linewidth is essentially in the low-temperature region. At such conditions there is no quantitative agreement, but the qualitative accordance occurs.

The pointed disagreement is easily explained by the simplicity of the proposed model. The real Fermi surface of aluminium has several sheets pertaining to different bands. At low temperatures in high purity metals the conduction electrons move on each Fermi surface sheet separately. Hence we must consider the real g anisotropy over the real Fermi surface to obtain adequate results. The same holds true not only for the temperature and frequency dependence of the CESR linewidth, but angular one as well.

Note, in case of conduction electron small-angle scattering predominance the equilibrium would be established separately within each of the Fermi surface hulls. This would require that the characteristic time of scattering leaving the conduction electron in its hull would be less than that of the interhull scattering. In this situation one could take advantage of a model involving several conduction electron groups.

To each of the electron groups one can ascribe such averaged characteristics as the g-factor, the spin relaxation time τ_s, the momentum relaxation time τ, and so on — depending on the model sophistication degree (see for instance a model proposed for Al in work [14]). This model involves three mechanisms of conduction electron connection: (1) conduction electron intergroup scattering with frequency $1/\tau_{ij}$, (2) exchange interaction, and (3) conduction electrons diffusive reflection from the boundary.

Note that in paper [4], dedicated to the CESR experimental research in Zn, the magnetic breakdown was pointed as a possible intergroup connection mechanism (see too [5, 6]).

Nevertheless, we think that the present model may be useful for qualitative understanding the spin relaxation processes connected with g anisotropy. The clear physical ideas lie in the model origin.

The model of reconstructed Fermi surface is possible to use in organic conductors in which intensive CESR investigations are carried out [7] and their Fermi surfaces consist of several sheets too. These materials are interesting for explorers from their superconducting properties with the transition temperature T_c up to 15 K [16].

We show, that in low and intermediate temperature the g-value anisotropy over Fermi sphere leads to the angular dependence of CESR linewidth. Unfortunately, as far as we know, there is no experimental data of angular dependence of CESR linewidth in Al. In works [17]–[24] only temperature dependence of CESR linewidth in mono- and polycrystal or the characteristics of the thin films were investigated.

Nevertheless, we believe that our model is qualitativy relevant to reality.

References

[1] Couch N.R., Sambles J.R., Stesmans A. and Cousins J.E. *J. Phys. F: Metal Phys.* **12**, 2439 (1982)

[2] Oseroff S., Gehman B.L. and Schultz S. *Phys. Rev. B* **15**, 1291 (1977); Braim S.P., Sambles J.R., Cousins J.E. *Sol.State Comm.* **28**, 981 (1978)

[3] Walker M.B. *Phys.Rev.Lett.* **33**, 406 (1974)

[4] Stesmans A. and Witters J. *Phys.Rev. B* **23**, 3159 (1983)

[5] Kochelaev B.I. and Proshin Yu.N. *Fiz. Tverd. Tela (Leningrad)* **27**, 265 (1985) (in Russian) [*Sov. Phys. Solid State.* **27**, 161 (1985)]

[6] Proshin Yu.N. and Useinov N.Kh. *Uspekhi Physicheskikh Nauk* **165**, 41 (1995) (in Russian) [*Physics-Uspekhi*, **38**, 39 (1995) (in English)]

[7] Kanoda K., *et al. Synth. Metals* **56**, 2309 (1993)

[8] Silsbee R.H. and Beuneu F. *Phys.Rev. B* **27**, 2682 (1983)

[9] Jafet J. *Sol. St. Phys.* **14**, 1 (1963)

[10] Bir G.L. and Pikus G.E. *Symmetry and Strain-Induced Effects in Semiconductors.* Wiley, New York (1975)

[11] Cracknell A.P and Wong K.C. *The Fermi surface.* Clarendon Press, Oxford (1973)

[12] Beuneu F. *J. Phys. F: Metal Phys.* **10**, 2875 (1980)

[13] Freedman R. and Fredkin D.R. *Phys.Rev. B* **11**, 4847 (1975)

[14] Silsbee R.H. and Long J.P. *Phys.Rev. B* **27**, 5734 (1983)

[15] Walker M.B. *Can. J. Phys. B* **53**, 165 (1975)

[16] Williams J.M., *et al. Science.* **252**, 1501 (1991)

[17] Lubzens D. and Shanabarger M.R., Schultz S. *Phys.Rev.Lett.* **29** 87 (1972)

[18] Janssens L., Stesmans A., Cousins J. E. and Witters J. *Phys. St. Sol.* B**67**, 231 (1975)

[19] Lubzens D. and Schultz S. *Phys.Rev.Lett.* **36** 1104 (1976)

[20] Dunifer G. L. and Pattison M. R., *Phys.Rev. B* **14**, 945 (1976)

[21] Dunifer G. L. and Pattison M. R., *Phys.Rev. B* **15**, 315 (1977)

[22] Sambles J. R. and Sharp-Dent G., Cousins J. E. *Phys. St. Sol.* B**79**, 645 (1977)

[23] J. van Meijel, Stesmans A., Cousins J. E. and Witters. J. *Sol.State Comm.* **21**, 753 (1977)

[24] Sambles J. R., Stesmans A., Cousins J. E. and Witters J. *Sol.State Comm.* **24**, 673 (1977)